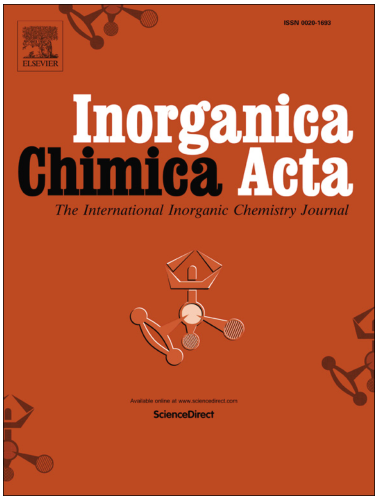

Research paper

Bis- Cyclometalated Rhodium- and Iridium- Complexes With the 4,4'-Dichloro-2,2'-Bipyridine Ligand. Evaluation of their Photophysical Properties and Biological Activity

Marion Graf, Yvonne Gothe, Nils Metzler-Nolte, Rafał Czerwieniec, Karlheinz Sünkel

PII: S0020-1693(17)30247-5
DOI: http://dx.doi.org/10.1016/j.ica.2017.04.006
Reference: ICA 17510

To appear in: *Inorganica Chimica Acta*

Received Date: 29 March 2017
Accepted Date: 3 April 2017

Please cite this article as: M. Graf, Y. Gothe, N. Metzler-Nolte, R. Czerwieniec, K. Sünkel, Bis- Cyclometalated Rhodium- and Iridium- Complexes With the 4,4'-Dichloro-2,2'-Bipyridine Ligand. Evaluation of their Photophysical Properties and Biological Activity, *Inorganica Chimica Acta* (2017), doi: http://dx.doi.org/10.1016/j.ica.2017.04.006

Bis- Cyclometalated Rhodium- and Iridium- Complexes With the 4,4’-Dichloro-2,2’-Bipyridine Ligand.
Evaluation of their Photophysical Properties and Biological Activity

Dedicated to Prof. Hans-Christian Böttcher on the Occasion of his 60th Birthday

Marion Graf[a], Yvonne Gothe[b], Nils Metzler-Nolte[b], Rafał Czerwieniec[c]
Karlheinz Sünkel[a*]

[a] *Department of Chemistry, Ludwig Maximilian University of Munich, Butenandtstraße 5–13, 81377 Munich, Germany*

[b]*Ruhr University of Bochum, Universitätsstraße 150, 44801 Bochum, Germany*

[c]*Institute of Physical and Theoretical Chemistry University of Regensburg, Universitätsstraße 31, 93053 Regensburg, Germany*

ABSTRACT

The synthesis and characterization of new cyclometalated complex salts [M(C^N)$_2$(4,4’-Cl$_2$bpy)]PF$_6$ (M = Rh and Ir; C^N = 2-(*p*-tolyl)pyridinato (**1** and **2**), 2-phenyl-5-chloro-pyridinato (**3** and **4**); 4,4’-Cl$_2$bpy = 4,4’-dichloro-2,2’-bipyridine) is described. Compounds **1** - **4** were obtained by reaction of 4,4’-dichloro-2,2’-bipyridine with the complexes [{M(µ-Cl)(C^N)$_2$}$_2$] (M = Rh, Ir) in refluxing CH$_2$Cl$_2$/MeOH mixtures. The molecular structures of compounds **1** and **4** were confirmed by X-ray diffraction. The Ir compounds show phosphorescence in PMMA film and in solution at ambient temperature. Furthermore, all compounds display significant cytotoxicity against human cancer cell lines with the IC$_{50}$ values in the 0.4 - 2 µM range.

KEYWORDS: Cyclometalated complexes; Rhodium; Iridium; phosphorescence; cytotoxicity

---

* Corresponding author. Tel.: +49 89218077773; fax: +49 89218077774
E-mail address: suenk@cup.uni-muenchen.de (K. Sünkel)

1. Introduction

Bis-cyclometalated Ir(III) complexes play an important role in the development of modern optoelectronic technologies (e.g. organic light emitting diodes − OLEDs and light-emitting electrochemical cells − LEECs), biological labels, and chemical sensors [1]. It was found by several groups that as well for LEEC's [2] as for sensoric applications [3], NLO materials[4] and bio-medical diagnostic and therapeutic studies [59] the use of water-soluble complexes of the type $[M(C\^{}N)_2(N\^{}N)]^+$ was particularly beneficial. Starting from the long-known compounds with M = Rh [10] and Ir [11], C^N = 2-phenylpyridinato (ppy) and N^N = 2,2'-bipyridine (bpy) or phenanthroline (phen), numerous studies were performed to elucidate the effects of various substituents on the photophysical and electrochemical properties of the complexes and how they influence the device performance in different applications [12-14]. Our group described a series of cyclometalated M(III) complexes (M = Rh, Ir) [15], including complexes containing biomolecules as the ancillary ligands [16].

Recently we found that the complexes $[M(ptpy)_2](ddpmp)]PF_6$ (M = Rh, Ir; ddmp = 4,7-dichloro-2,9-dimethyl-1,10-phenanthroline)), which contain chloro-substituents on the pyridine parts of the phenanthroline ligand, showed promising luminescence and cytotoxic properties [17]. In this paper we describe the synthesis and characterization of four new cyclometalated complex salts $[M(C\^{}N)_2(4,4'\text{-}Cl_2bpy)]PF_6$ which contain the structurally related 4,4'-dichloro-2,2'-bipyridine ligand, which was also studied before in a Rh(I) complex [18] for catalytic properties, a Ru(II) complex [19] as agent against tuberculosis or a Rh(III) complex [20] for indirect electrochemical cofactor regeneration.

2. Experimental

2.1. General considerations

All manipulations were performed under an atmosphere of dry nitrogen using conventional Schlenk techniques. 4,4'-dichloro-2,2'-bipyridine (Aldrich), 2-(*p*-tolyl)pyridine (Aldrich), 5-chloro-2-phenyl-pyridine (Synchem) were used as received.

$[\{M(\mu\text{-}Cl)(C\^{}N)_2\}_2]$ (M = Rh, Ir) were prepared by adequately modified literature methods [15b, e]. NMR spectra were usually recorded in CD_2Cl_2 using a Jeol Eclipse 400 instrument operating at 400 MHz (^1H) and 100 MHz (^{13}C) respectively. Chemical shifts are given in ppm, referenced to the solvent signals at $\delta = 5.30$ (^1H) or 53.8 ppm (^{13}C). Mass spectra were measured using a Jeol Mstation JMS 700 spectrometer. Elemental analyses (C, H, N) were performed by the Microanalytical Laboratory of the Department of Chemistry, LMU Munich, using a Heraeus Elementar Vario EL instrument.

Dulbecco's Modified Eagle's Medium (DMEM), containing 10% fetal calf serum, 1% penicillin and streptomycin, was used as growth medium. MCF-7 and HT-29 cells were detached from the wells with trypsin and EDTA, harvested by centrifugation and resuspended again in the cell culture medium. The assays were carried out on 96 well plates with 6000 (3000) cells per well for MCF-7 (HT-29, respectively). After 24 h of incubation at 37°C and 10% CO_2, the cells were treated with the compounds **1** and **2** (with DMSO concentrations of 0.5%) with a final volume of 200 µl per well. For a negative control, one series of cells was left untreated. The cells were incubated for 48 h followed by adding 50 µl MTT (2.5 mg/ml). After an incubation time of 2 h, the medium was removed and 200 µl DMSO were added. The formazan crystals were dissolved and the absorption was measured at 550 nm, using a reference wavelength of 620 nm. Each test was repeated in quadruplicates in two independent experiments for each cell line.

2.2. Starting Materials

2.2.1. [{Ir(µ-Cl)(5-Cl-ppy)$_2$}$_2$]

Yield: 440 mg (65.5 %). *Anal.* Calc. for $C_{44}H_{28}Cl_6Ir_2N_4$: C, 43.68; H, 2.33; N, 4.63 Found: C, 44.04; H, 2.57; N, 4.51 %. MS (FAB^+): *m/z* = 1210.5 $[M+H]^+$, 604.3 $[M/2^+]$. ^1H NMR: δ 9.14 (d, *J* = 6.3 Hz, 4 H), 7.95 (d, *J* = 2.3 Hz, 4 H), 7.54 (dd, *J* =7.9/ 1.2 Hz, 4 H), 6.91 (dd, *J* = 6.3/ 2.3 Hz, 4H), 6.89-6.83 (m, 4H), 6.68 (td, *J* =7.5/ 1.3 Hz, 4 H), 5.95 (dd, *J* =7.8/ 1.1 Hz, 4H). ^{13}C {^1H} NMR (100 MHz, $CDCl_3$): δ 169.7, 151.1, 145.3, 145.1, 142.7, 130.6, 130.1, 124.4, 122.4, 122.0, 119.1.

2.2.2. [{Rh(µ-Cl)(5-Cl-ppy)$_2$}$_2$]

Yield: 45 mg (31.5 %). *Anal.* Calc. for $C_{44}H_{28}Cl_6N_4Rh_2$: C, 51.24; H, 2.74; N, 5.43. Found: C, 51.31; H, 3.06; N, 5.00 %. MS (FAB^+): *m/z* = 1033 $[M^++2H]$, 516 $[M/2^+]$, 479 $[M/2^+-Cl]$. ^1H NMR: δ 9.09 (m, 4 H), 7.93 (d, *J* = 2.4 Hz, 4 H), 7.58 (dd, *J* = 7.8/ 1.4 Hz, 4 H), 6.92 (m, 4H), 6.88 (dt, *J* = 6.2/ 2.3 Hz, 4H), 6.74 (dt, *J* = 7.6/ 1.4 Hz, 4H), 5.96 (d, *J* = 7.2 Hz, 4H). ^{13}C {^1H} NMR: δ 166.68/ 166.66, 166.3 (d, J_{RhC} = 36,6 Hz), 152.9, 145.9, 143.0, 132.4, 130.27/ 130.25, 124.50/ 124.49, 123.2, 122.66/122.65, 119.67/ 119.66.

*2.3. Synthesis of [Rh(ptpy)$_2$(4,4'Cl$_2$bpy)]PF$_6$ (**1**)*

To a solution of [{Rh(µ-Cl)(ptpy)$_2$}$_2$] (142 mg, 0.15 mmol) in 25 mL of CH_2Cl_2/ MeOH (1v: 1v) 4,4'-Cl_2bpy = 4,4'-dichloro-2,2'-bipyridine (90 mg, 0.4 mmol) was added and the mixture refluxed with stirring for 2 h. After cooling to room temperature, KPF_6 (70 mg, 0.4 mmol) was added. The solvent was removed to dryness in vacuo and the residue dissolved in dichloromethane and chromatographed on alumina with CH_2Cl_2/ acetone (9:1) as the eluent. The solution was evaporated to dryness and the residue was redissolved in 5 ml of dichloromethane and **1** was crystallized by slow diffusion of *n*-hexane.

Yield: 142 mg (58.4%). *Anal*. Calc. for $C_{34}H_{26}Cl_2F_6N_4PRh$: C, 50.45; H, 3.24; N, 6.92. Found: C, 50.78; H, 3.48; N, 6.50 %. MS (FAB$^+$): m/z = 663.4 [M$^+$] complex cation. ^{1}H NMR (400 MHz, CD_2Cl_2): δ 8.36 (d, J= 1.9 Hz, 2 H), 7.95 (d, J= 5.8 Hz, 2 H), 7.91 (d, J= 7.8 Hz, 2 H), 7.88- 7.83 (m, 2 H), 7.68 (d, J= 7.9 Hz, 2 H), 7.50 (dd, J= 5.8/ 1.8 Hz, 2 H), 7.46 (d, J= 5.8 Hz, 2 H), 7.07- 7.01 (m, 2H), 6.96 (d, J= 8.4 Hz, 2 H), 6.09 (s, 2H), 2.13 (s, 6 H). ^{13}C {^{1}H} NMR (400 MHz, CD_2Cl_2): δ 166.4 (d, J_{RhC} = 32Hz), 165.18/165.17, 154.9, 151.4, 148.8, 148.7, 141.47/141.46, 141.2, 138.8, 133.7, 128.8, 125.3, 125.00, 124.99, 123.39/ 123.38, 120.17/120.15, 21.6.

*2.4. Synthesis of [Ir(ptpy)$_2$(4,4'-Cl$_2$bpy)]PF$_6$ (**2**)*

To a solution of [{Ir(μ-Cl)(ptpy)$_2$}$_2$] (169 mg, 0.15 mmol) in 25 mL of a mixture of CH_2Cl_2/MeOH (1:1) the ligand 4,4'-Cl$_2$bpy = 4,4'-dichloro-2,2'-bipyridine (90 mg, 0.4 mmol) was added and the mixture refluxed with stirring for 2 h. After cooling to room temperature KPF_6 (70 mg, 0.38 mmol) was added. The solvent was removed in vacuo and the residue was dissolved in dichloromethane and chromatographed on alumina with CH_2Cl_2/acetone (9:1) as the eluent. The solution was evaporated to dryness and the residue redissolved in 5 ml of dichloromethane. The product was precipitated by slow diffusion of hexane. Suitable crystals for X-ray diffraction were obtained by slow diffusion of hexane into a solution of dichloromethane/chloroform at room temperature.

Yield: 142 mg (52.7 %). *Anal*. Calc. for $C_{34}H_{26}Cl_2F_6IrN_4P$: C, 45.44; H, 2.92; N, 6.23. Found: C, 44.91; H, 3.09; N, 5.87 %. MS (FAB$^+$): m/z = 753.3 [M$^+$] complex cation. ^{1}H-NMR: δ 8.36 (d, J= 2 Hz, 2 H), 7.90 (m, 4 H), 7.75 (m, 2 H), 7.60 (d, J= 12 Hz, 2 H), 7.44 (m, 4 H), 6.97 (m, 2 H), 6.88 (d, J= 8 Hz, 2 H), 6.05 (s, 2 H), 2.13 (s, 6 H). ^{13}C {^{1}H} NMR: δ 167.6, 166.0, 151.5, 149.0 148.4, 147.8, 141.4, 140.9, 138.3, 132.3, 132.3, 129.1, 125.3, 124.9, 124.0, 123.0, 119.6, 21.5.

*2.5. Synthesis of [Rh(5-Cl-ppy)$_2$(4,4'Cl$_2$bpy)]PF$_6$ (**3**)*

To a solution of [{Rh(μ-Cl)(5-Cl-ppy)$_2$}$_2$] (155 mg, 0.15 mmol) in 20 mL of a mixture of CH_2Cl_2/MeOH (1:1), the ligand 4,4'-Cl_2bpy = 4,4'-dichloro-2,2'-bipyridine (68 mg, 0.3 mmol) was added and the mixture was stirred and refluxed for 2 hours. After cooling to room temperature KPF_6 (74 mg, 0.4 mmol) was added. The solvent was removed in vacuo and the residue was dissolved in dichloromethane and chromatographed on alumina with CH_2Cl_2/acetone (9:1) as the eluent. Crystals were obtained by slow diffusion of isohexane into a solution in dichloromethane/chloroform at room temperature.

Yield: 141.3 mg (55 %). *Anal.* Calc. for $C_{32}H_{20}Cl_4F_6N_4PRh$: C, 45.21; H, 2.37; N, 6.59. Found: C, 45.21; H, 2.72; N, 6.43 %. MS (FAB$^+$): m/z = 705.2 [M$^+$] complex cation.

^{1}H NMR: δ= 8.39 (d, *J*= 2.0 Hz, 2 H), 7.95 (d, *J*= 2.2 Hz, 2 H), 7.89 (d, *J*= 5.7 Hz, 2 H), 7.74 (d, *J*= 7.3 Hz, 2 H), 7.51 (dd, J= 5.8/ 2.0 Hz, 2 H), 7.46 (d, *J*= 6.2 Hz, 2 H), 7.16 (t, *J*= 7.5 Hz, 2 H), 7.12 (dd, *J*= 6.2/ 2.2 Hz, 2 H), 7.08-7.02 (m, 2 H), 6.36 (d, *J*= 7.6 Hz, 2 H).

^{13}C {^{1}H} NMR : δ= 166.5 (d, J_{RhC}= 32 Hz), 166.03/166.01, 154.8, 151.2, 149.9, 149.0, 147.5, 142.8, 133.1, 131.63/131.61, 129.0, 125.5, 125.4, 124.5, 124.4, 120.82/120.81.

*2.6. Synthesis of [Ir(5-Cl-ppy)$_2$(4,4'-Cl$_2$bpy)]PF$_6$ (**4**)*

To a solution of [{Ir(μ-Cl)(5-Cl-ppy)$_2$}$_2$] (181.5 mg, 0.15 mmol) in 20 mL of a mixture of CH_2Cl_2/ MeOH (1:1), the ligand 4,4'-Cl_2bpy = 4,4'-dichloro-2,2'-bipyridine (68 mg, 0.3 mmol) was added and the mixture was stirred and refluxed for 2 hours. After cooling to room temperature KPF_6 (70 mg, 0.38 mmol) was added. The solvent was removed in vacuo and the residue was dissolved in dichloromethane and chromatographed on alumina with CH_2Cl_2/ acetone (9:1) as the eluent. Suitable crystals for X-ray diffraction were obtained by slow diffusion of isohexane into a solution in dichloromethane/chloroform at room temperature.

Yield: 160.5 mg (57 %). *Anal.* Calc. for $C_{32}H_{20}Cl_4F_6IrN_4P$: C, 40.91; H, 2.15; N, 5.96. Found: C, 40.61; H, 2.33; N, 5.69 %. MS (FAB$^+$): m/z = 793.4 [M$^+$] complex cation.

^{1}H-NMR: δ = 8.41 (d, *J*= 2.1 Hz, 2 H), 7.94 (d, *J* = 2.2 Hz, 2 H), 7.86 (d, *J* = 5.9 Hz, 2 H), 7.70 (dd, *J* = 7.9/ 1.1 Hz, 2 H), 7.50 (dd, *J*= 5.9/ 2.1 Hz, 2 H), 7.47 (dd, J= 6.3/ 0.5 Hz, 2 H), 7.15- 7.05 (m, 4 H), 6.99 (td, *J*= 7.4/ 1.3 Hz, 2 H), 6.33 (dd, *J*= 7.6/ 0.7 Hz, 2H).

^{13}C {^{1}H} NMR: δ= 168.8, 156.0, 151.4, 149.5, 149.0, 148.3, 146.9, 142.5, 131.8, 131.6, 129.3, 125.7, 125.5, 124.0, 123.3, 120.3.

2.7. X-ray structural determinations

A suitable single crystal of **1** was selected by means of a polarization microscope, mounted on the tip of a glass fiber, and investigated on a BRUKER D8 Venture diffractometer using Mo-Kα radiation (λ = 0.71073 Å). The crystal turned out to be a racemic twin, containing two symmetry-independent molecules in the asymmetric unit. The intensities were corrected for absorption by the semi-empirical multiscan method (SADABS). The structure was solved by direct methods (SIR 97) using a HKLF4 file and refined by full-matrix least-squares calculations on F^2 (SHELXL-2014/7) using a HKLF5 file with BASF= 0.268, as implemented in the software package WINGX. [21] Refinement turned out to be rather difficult, as the compound co-crystallized with CH_2Cl_2, MeOH and water, which could be localized (however, severely disordered) and refined using several restraints. Even then, analysis by PLATON showed the presence of 4.8% solvent accessible voids. Anisotropic displacement parameters were refined for all non-hydrogen atoms except the carbon and oxygen atoms of the disordered solvent molecules.

Crystals of **4** suitable for an X-ray diffraction study were grown from $CH_2Cl_2/CHCl_3$/hexane solutions. Data collection, structure solution (SIR 97) and refinement (SHELXL-2014/7) could be performed without any problems. There were neither co-crystallized solvents nor any residual solvent accessible voids.

Details of the crystal data, data collection, structure solution, and refinement parameters are summarized in Table 1.

2.8. Photophysical Measurements.

UV-Vis absorption spectra were recorded with a Varian Cary 300 double beam spectrometer. Luminescence spectra were measured with a Horiba Jobin Yvon Fluorolog 3 steady-state fluorescence spectrometer. For decay time measurements a PicoQuant LDH-P-C-375 pulsed diode laser (λ_{exc} = 372 nm, pulse width 100 ps) was applied as the excitation source. The emission signal was detected with a cooled photomultiplier attached to a FAST ComTec multichannel scalar card with a time resolution of 250 ps. Photoluminescence quantum yields were determined with a Hamamatsu C9920-02 system equipped with a Spectralon® integrating sphere. Diluted solutions ($c \approx 10^{-5}$ M^{-1}) in dichloromethane (CH_2Cl_2) were degassed by several freeze-pump-thaw cycles ($p = 1\times10^{-5}$ mbar). Polymer films containing about 0.1 weight% of the Ir complex were obtained by dissolving the emitter and poly(methyl methacrylate) (PMMA) in dichloromethane and spin-coating this solutions onto quartz glass substrates. PMMA films were measured under continuous flushing with nitrogen.

Table 1: Crystal data and structure refinement details for **1** and **3**.

Compound	**1**	**4**
Empirical formula	$C_{35.75}H_{30.5}Cl_{4.5}F_6N_4OPRh$	$C_{32}H_{20}Cl_4F_6IrN_4P$
Formula weight	939.55	939.49
Temperature [K]	100(2)	173(2)
Crystal system	Monoclinic	
Space group	P 2_1	P 2_1/n
Unit cell dimensions		
a [Å]	11.6660(6)	9.4737(3)
b	25.4895(14)	13.8553(4
c	14.1754(8) Å	24.5688(8)
ß [°]	93.879(2).	93.509(3)
Volume [$Å^3$]	4205.5(4)	3218.88(17)
Z	2x2	4
Density (calc., [g/cm^3])	1.484	1.939
Absorption coefficient	0.790 mm^{-1}	4.597
F(000)	1886	1816
Crystal size [mm^3]	0.08 x 0.04 x 0.03	0.279 x 0.118 x 0.07
Theta range for data collection	2.881 to 26.453°.	4.31 to 26.37°.
Index ranges	-14≤h≤14, 0≤k≤31, 0≤l≤17	-11≤h≤11, -15≤k≤17, -19≤l≤30
Reflections collected	11822	20539
Independent reflections	11822	6559 [R(int) = 0.0426]
Completeness	99.7 %	99.6 %
Max. and min. transmission	0.7454 and 0.693	1 and 0.84257
Data / restraints / parameters	11822 / 17 / 949	6559 / 0 / 433
Goodness-of-fit on F^2	1.125	1.086
Final R indices [I>2sigma(I)]	R1 = 0.0540, wR2 = 0.1271	R1 = 0.0529, wR2 = 0.1325
R indices (all data)	R1 = 0.0631, wR2 = 0.1323	R1 = 0.0618, wR2 = 0.1389
Absolute structure parameter	0.05(5)	-
Largest diff. peak and hole [e.$Å^{-3}$]	1.381 and -0.626	4.992 and -1.278

2.9. Computational Methodology.

Molecular geometries and electronic structures of [Rh(ptpy)$_2$(4,4'-Cl$_2$bpy)]PF$_6$ and [Ir(ptpy)$_2$(4,4'-Cl$_2$bpy)]PF$_6$ were calculated using the density functional theory (DFT) with the hybrid gradient corrected correlation functional B3LYP [22]. The Ahlrichs split-valence basis set SVP [23] was applied for atoms C, H, N, and Cl and the quadruple-zeta quality basis set QZVP [24] was used for Rh and Ir atoms. Inner-core electrons of Rh and Ir were substituted with relativistic effective core potentials. [25] TD-DFT calculations for $[Ir(ptpy)_2(4,4'-Cl_2bpy)]^+$ (**2**) were performed in the optimized ground state geometry using the same B3LYP functional and basis sets. Ten lowest singlet and triplet excitations were computed. All computations were carried out using the Gaussian 09 program package.[26]

2.10. Cell culture and cytotoxicity.

Dulbecco's Modified Eagle's Medium (DMEM), containing 10% FCS, 1% penicillin and streptomycin, was used as growth medium. MCF-7 and HT-29 cells were detached from the wells with trypsin and EDTA, harvested by centrifugation and re-suspended in cell culture medium. The assays have been carried out on 96 well plates with 6000 cells per well for both cell lines. After 24 h of incubation at 37°C and 10% CO_2, the cells were treated with the compounds (with DMSO concentrations of 0.5%) with a final volume of 200 µl per well. For the negative control, one series of cells was left untreated. The cells were incubated for 48 h followed by adding 50 µl MTT (2.5 mg/ml). After an incubation time of 2 h, the medium was removed and 200 µl DMSO were added. The formazan crystals were dissolved and the absorption was measured at 550 nm, using a reference wavelength of 620 nm. Each test was repeated in triplicates or quadruplicates in at least three independent experiments for each cell line.

3. Results and discussion

3.1. Synthesis and characterization of compounds

The cyclometalating ligands 2-*para*-tolyl-pyridine ("Hptpy") and 5-Chloro-2-phenylpyridine ("HClppy") were used for the synthesis of the chloro-bridged dimers $[\{M(\mu\text{-}Cl)(C^\wedge N)_2\}_2]$ (M = Rh, Ir; C^N= ptpy, ClPppy) starting from the corresponding M(I) complexes $[\{M(\mu\text{-}Cl)(coe)_2\}_2]$ by an oxidative addition reaction as described previously [15b, e]. Subsequently, the preparation of the cationic mononuclear title complexes was started by cleavage of these dimeric compounds by the chelating ligand 4,4'-Cl_2bpy = 4,4'-dichloro-2,2'-bipyridine in a refluxing mixture of dichloromethane/methanol. The primarily formed chloride salts $[M(C^\wedge N)_2(4,4'-Cl_2bpy)]Cl$ yielded after metatheses with KPF_6 the hexafluorophosphate derivatives **1** – **4** (see *Scheme 1*). All compounds were obtained as yellow crystals in good yields and were characterized by elemental analyses, ^1H and ^{13}C NMR spectroscopy, mass spectrometry and additionally for **1** and **4** by single crystal X-ray diffraction studies.

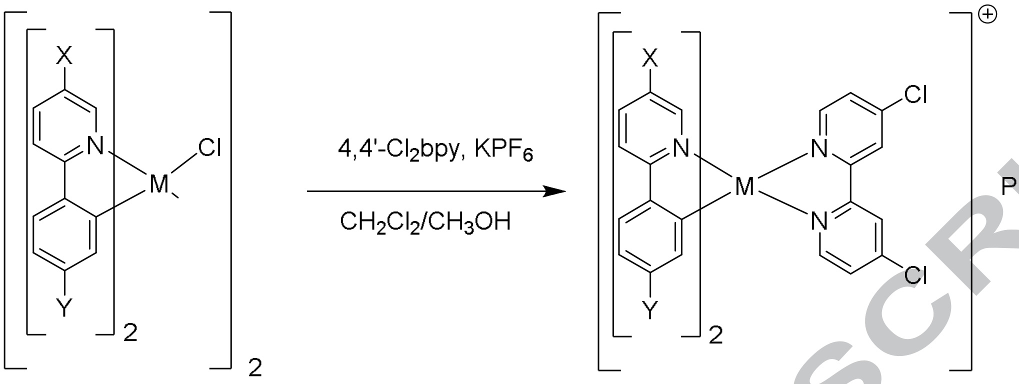

	1	**2**	**3**	**4**
M	Rh	Ir	Rh	Ir
X	H	H	Cl	Cl
Y	CH_3	CH_3	H	H

Scheme 1: Synthesis of compounds **1**–**4**

3.2. Crystal and molecular structures of **1** *and* **4**

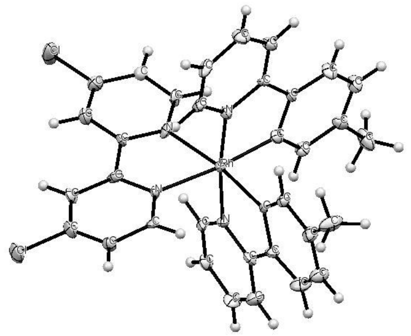

Figure 1: Molecular Structure of the cation of compound **1**; shown is the isomer with Δ configuration

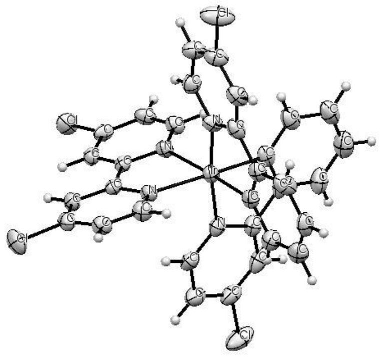

Figure 2: Molecular Structure of the cation of compound **4**; shown is the Λ isomer

ORTEP drawings of both compounds can be seen in *Figures* 1 and 2. Compound **1** crystallized unfortunately as a racemic twin with disordered solvent molecules in approximate stoichiometry $(\mathbf{1})_4(CH_2Cl_2)_5(MeOH)_2(H_2O)_2$. The unit cell contains two symmetry-independent molecules of **1,** one with Δ- configuration and one with Λ configuration on Rh.

The nitrogen atoms of the cyclometalating ligands are in a mutual trans- configuration, as usually observed. The bond parameters (in Å and °) involving the metal atoms are collected in Table 2. As can be seen there, these parameters are for both independent molecules identical within the 2σ criterion. The bonds from rhodium to the bpy nitrogen atoms are by ca. 0.1Å longer than to the nitrogen atoms of the cyclometallating ligands, which is presumably due to the *trans* influence of the Rh-C bonds. Very similar parameters were observed in the related thienyl-pyridine complex [Rh(thpy)$_2$(bpy)]Cl, (comp."A" in Table 2) [10c]. The planes of the two pyridine rings of the bpy ligand are slightly twisted (4.4° and 8.0°).

Compound **4** crystallizes with no solvents in the centrosymmetric space group P2$_1$/n with only one independent molecule in the asymmetric unit. Again, the nitrogen atoms of the cyclometallating ligands are in mutual trans configuration. Bond parameters around the central iridium atom are collected again in Table 2. Again, the bond lengths from the metal to the bpy nitrogen atoms are longer than those to the Clppy nitrogen atoms, but somewhat surprising, they are actually slightly shorter than the corresponding bond lengths of the rhodium compound. However, similar distances and angles were reported for the related [Ir(ppy)$_2$(bpy)]PF$_6$ (comp. "B" in Table 2) [2c]. The planes of the two halves of the bipy ligand are again slightly twisted by 7°, while in B this torsion angle amounts only to 1.4°.

Table 2: Bond geometries around the metal atoms in **1** and **4** and two related complexes.

	M-N$_{bpy}$	M-N$_{C^N}$	M-C$_{C^N}$	(N-M-N)$_{bpy}$	(N-M-C)$_{C^N}$	(N-M-N')$_{C^N}$	C-M-N$_{bpy}$
1 (mol. 1)	2.158(11) 2.153(10)	2.023(10) 2.061(10)	1.998(12) 2.012(10)	75.5(4)	80.5(5) 81.6(4)	173.3(4)	173.8(6) 171.8(5)
1 (mol. 2)	2.156(10) 2.175(9)	2.050(10) 2.038(11)	2.013(10) 1.988(14)	75.0(4)	82.2(5) 81.3(5)	172.9(4)	171.6(5) 174.0(5)
A	2.145(3) 2.138(4)	2.055(4) 2.065(4)	1.984(4) 1.993(5)	76.7(1)	80.7(2) 81.1(2)	170.7(1)	173.6(2) 173.7(2)
4	2.136(6) 2.136(6)	2.054(6) 2.021(6)	2.031(8) 2.015(7)	76.1(2)	79.7(3) 80.1(3)	172.9(3)	172.8(3) 175.6(3)
B	2.129 2.136	2.047 2.042	2.024 2.004	76.20	80.68 80.02	172.09	171.92 171.90

3.3. Photophysical properties

UV-Vis absorption spectra were studied in dichloromethane (c = 0.05 mM) at room temperature. Absorption maxima for both Rh and Ir complexes are listed in Table 3 (below). The respective spectra of [Rh(ptpy)$_2$(4,4'-Cl$_2$bpy)]PF$_6$ (**1**) and [Ir(ptpy)$_2$(4,4'-Cl$_2$bpy)]PF$_6$ (**2**) are shown in Fig. 3. With reference to previous studies on related complexes [1c, 17, 27–31] the higher-energy intense bands occurring at $\lambda_{abs} \leq 330$ (with maximum molar absorption coefficients ε in the order of 10^4 M^{-1}cm^{-1}) nm are assigned to spin-allowed ligand-centered π

→ π* transitions of the ptpy and 4,4’-Cl_2bpy ligands. In the lower energy region, between 330 and 400 nm for [Rh$(ptpy)_2$(4,4’-Cl_2bpy)]PF_6 (**1**) and 330 – 450 nm for [Ir$(ptpy)_2$(4,4’-Cl_2bpy)]PF_6 (**2**), respectively, weaker absorption bands (ε in the order of several thousand $M^{-1}cm^{-1}$) are observed. Since such absorptions are not displayed by the free ligands ptpyH and 4,4’-Cl_2bpy, the long-wavelength absorption bands of the Rh and Ir complexes are assigned to metal-to-ligand charge-transfer (MLCT) transitions involving the occupied d_π orbitals of the metals ($4d_\pi$(Rh) and $5d_\pi$(Ir) in [Rh$(ptpy)_2$(4,4’-Cl_2bpy)]PF_6 (**1**) and [Ir$(ptpy)_2$(4,4’-Cl_2bpy)]PF_6 (**2**), respectively) and empty π* orbitals of the ptpy and 4,4’-Cl_2bpy ligands. The significant red-shift of the MLCT absorptions in the Ir complex as compared to the Rh congener is readily accounted for the higher energy of the occupied d orbitals of the $5d^6$ ion Ir^{3+} than in the $4d^6$ ion Rh^{3+}, respectively.

The above assignments are further supported by results of the TD-DFT calculations. In particular, the frontier orbitals of [Ir$(ptpy)_2$(4,4’-Cl_2bpy)$]^+$ (**2**) drawn in Fig. 3 involve different regions of the molecule. As analyzed in Table 3, The HOMO is largely composed of a $5d_\pi$ atomic orbital of Ir with significant admixtures of the π (ptpy) character and the LUMO (π*) is largely centered on the 4,4’-Cl_2bpy ligand. Since the lowest energy transitions $S_0 \rightarrow T_1$ and $S_0 \rightarrow S_1$ result mainly from the HOMO→LUMO excitation, distinct charge-transfer character ($5d_\pi$(Ir)→ π*(4,4’-Cl_2bpy)) of the lowest excited states is predicted.

Table 3. Percent contributions of Ir, ptpy, and 4,4’-Cl_2bpy to selected highest occupied lowest virtual molecular orbitals of [Ir$(ptpy)_2$(4,4’-Cl_2bpy)$]^+$ (**2**). The Mulliken population analysis was performed for the ground-state Kohn-Sham orbitals resulting from the B3LYP/{SVP+QZVP(ECP)} DFT calculations using the Chemissian computer program [32

Orbital	Energy (eV)	Ir (%)	ptpy1 (%)	ptpy2 (%)	4,4’-Cl_2bpy (%)
HOMO – 5	-9.018	40	27	27	6
HOMO – 4	-8.920	64	15	15	5
HOMO – 3	-8.874	28	33	33	5
HOMO – 2	-8.661	16	41	41	-
HOMO – 1	-8.468	5	47	47	-
HOMO	-7.942	35	32	32	2
LUMO	-5.439	3	-	-	96
LUMO + 1	-4.616	3	2	2	93
LUMO + 2	-4.347	1	2	2	95

LUMO + 3	-4.222	5	47	47	1
LUMO + 4	-4.142	4	46	46	4
LUMO + 5	-3.718	3	47	47	4

Table 4. Vertical transition energies, oscillator strengths, and orbital character of three lowest energy electronic transitions of $[Ir(ptpy)_2(4,4'\text{-}Cl_2bpy)]^+$ (**2**) resulting from TD-DFT computations on the B3LYP/[SVP+QZVP(ECP)] level of theory.

Transition	Energy /eV	Oscillator strength	Main contributions	Natural transition orbitals [33] hole	Natural transition orbitals [33] electron
$S_0 \rightarrow T_1$	1.809	0	HOMO→LUMO (96 %)	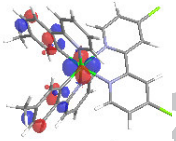	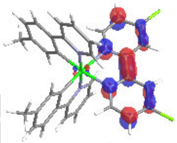
$S_0 \rightarrow T_2$	2.406	0	HOMO-5→LUMO (64 %) HOMO-3→LUMO (16 %) HOMO-1→LUMO (16 %)	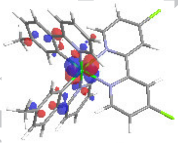	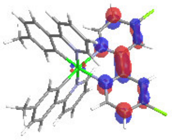
$S_0 \rightarrow T_3$	2.474	0	HOMO-4→LUMO (55 %) HOMO-2→LUMO (40 %)	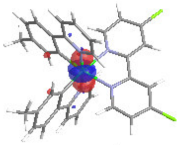	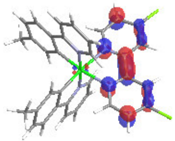
$S_0 \rightarrow S_1$	1.837	0.0002	HOMO→LUMO (98 %)	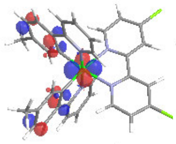	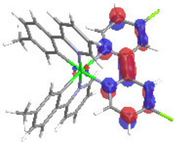
$S_0 \rightarrow S_2$	2.509	0.0105	HOMO-1→LUMO (98 %)	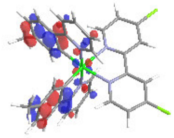	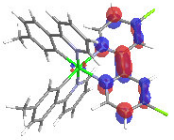
$S_0 \rightarrow S_3$	2.580	0.0006	HOMO-4→LUMO (61 %) HOMO-2→LUMO (38 %)	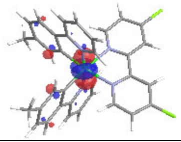	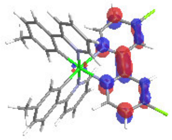

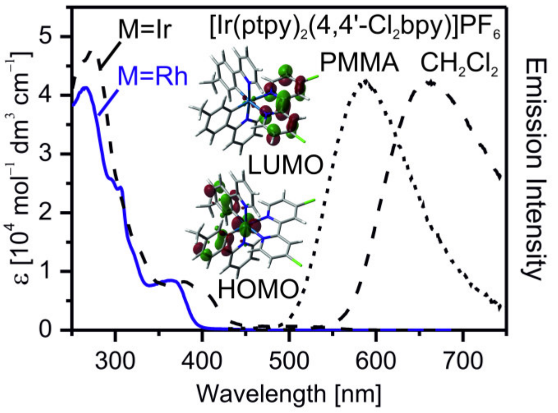

Figure 3. UV-Vis absorption and room-temperature luminescence spectra of [M(ptpy)$_2$(4,4'-Cl$_2$bpy)]PF$_6$. M = Rh (**1**): Blue solid line (solvent CH$_2$Cl$_2$). M = Ir (**2**): Black dashed lines (solvent CH$_2$Cl$_2$) and dotted line (PMMA matrix).

The iridium complexes [Ir(ptpy)$_2$(4,4'-Cl$_2$bpy)]$^+$ (**2**) and [Ir(5-Cl-ppy)$_2$(4,4'-Cl$_2$bpy)]$^+$ (**4**) are luminescent in solution and in organic polymer matrices. (Fig. 3 and Table 5) In dichloromethane at ambient temperature, they show weak red emission centered at 660 nm (**2**) and 643 nm (**4**) with the quantum yields ϕ_{PL} of 3 and 6 %, respectively. The decay times τ are 60 and 50 ns, respectively. In poly(methyl methacrylate) (PMMA), the emissions with maxima at λ_{em} = 580 nm (**2**) and 560 nm (**4**) are significantly blue shifted relative to the liquid solution. The quantum yields and emission decay times increase by about 10 times to ϕ_{PL} = 32 % and τ = 900 ns for [Ir(ptpy)$_2$(4,4'-Cl$_2$bpy)]$^+$ (**2**) and ϕ_{PL} = 60 % and τ = 950 ns for, [Ir(5-Cl-ppy)$_2$(4,4'-Cl$_2$bpy)]$^+$ (**4**), respectively. The relatively small radiative rates calculated according to

$k_r = \phi_{PL}/\tau$,

being $k_r = 3.6 \times 10^5$ s^{-1} for **2** and $k_r = 6.3 \times 10^5$ s^{-1} for **4**, respectively, point to a spin forbidden character of the corresponding electronic transitions. Thus, the emitting state is assigned as the lowest triplet state ^{3}MLCT (5d$_\pi$(Ir)$\rightarrow$ π*(4,4'-Cl$_2$bpy)). However, the k_r values are still relatively high as for phosphorescence. A corresponding allowedness is results from strong spin-orbit coupling of the lowest triplet state to the higher ^{1}MLCT singlet states. (cf. [1c ,34].)

Rigidochromic effects similar to those described above for [Ir(ptpy)$_2$(4,4'-Cl$_2$bpy)]$^+$ (**2**) and [Ir(5-Cl-ppy)$_2$(4,4'-Cl$_2$bpy)]$^+$ (**4**), such as the spectral blue shift and increase of ϕ_{PL} and τ when liquid solution (CH$_2$Cl$_2$) is replaced with a rigid polymer matrix (PMMA), were already reported for analogous luminescent iridium complexes. [17,29,31,35,36] Thus, the observed emission enhancement in rigid PMMA matrix as compared to the liquid CH$_2$Cl$_2$ solution can be accounted for different electrostatic interactions of the ^{3}MLCT-excited molecule with the induced dipole moments in its close surrounding. In solution, the solute-solvent rearrangements lead to significant stabilization of the ^{3}MLCT excited state and, thus, to a lower emission energy (longer wavelength; λ_{em} = 660 nm (for **2**) in CH$_2$Cl$_2$). As a consequence, vibrational coupling between the emitting ^{3}MLCT state and the ground state increases leading, according to the energy-gap law [1c ,37], to more effective non-radiative relaxation manifested by distinctly lower ϕ_{PL} and τ_{em} values. On the contrary, in PMMA such reorganizations are largely suppressed. Thus, non-radiative relaxation of the apparently blue-shifted emission (λ_{em} = 580 nm (for **2**) in PMMA) becomes less important and the ϕ_{PL} and τ_{em} values remain large.

Table **5.** UV-vis absorption and luminescence data[a] for complexes **1** – **4** at ambient temperature.

Complex	**1**	**2**	**3**	**4**
λ_{abs} [nm], ε [10^4 $M^{-1}cm^{-1}$] in parentheses. (CH_2Cl_2)	365 (0.9); 266 (4.1)	390 (0.8); 273 (4.6)	373 (0.9); 266 (5.5)	380 (0.8); 275 (4.6)
λ_{em} [nm] (CH_2Cl_2)	-	660	-	643
ϕ_{PL} [%] (CH_2Cl_2)	-	3	-	6
τ_{em} [ns] (CH_2Cl_2)	-	60	-	50
λ_{em} [nm] (PMMA)	-	580	-	560
ϕ_{PL} [%] (PMMA)	-	32	-	60
τ_{em} [ns] (PMMA)	-	900	-	950

a) λ_{abs} = absorption maximum, ε = molar absorption coefficient, λ_{em} = emission maximum, ϕ_{PL} = emission quantum yield, and τ_{em} = emission decay time, respectively.

3.5. Biological activity.

Several cyclometalated Ir(III) and Rh(III) complexes not only show strong luminescence, but also manifest encouraging antiproliferative properties both *in vitro* and *in vivo*. For this reason, the antiproliferative activity of the complexes towards the cancer cell lines MCF-7 (human breast adenocarcinoma) and HT-29 (colon adenocarcinoma) has been evaluated using the MTT assay. The resulting IC_{50} values are shown in Table 4.

Table 4 Antiproliferative effects of complexes **1** – **4** in MCF-7 and HT-29 cells. IC_{50} values are expressed as means [µM] (± standard deviation) of three independent experiments. Numbers are reported to two relevant digits in all cases for consistency, thus resulting in apparently different precision

IC_{50}/µM

Compound	HT-29	MCF-7
[Rh(ptpy)$_2$(Cl$_2$-bpy)]PF$_6$ (**1**)	0.41 ± 0.21	2.37 ± 0.81
[Ir(ptpy)$_2$(Cl$_2$-bpy)]PF$_6$ (**2**)	0.55 ± 0.19	1.43 ± 0.21

[Rh(Cl-ptpy)$_2$(Cl$_2$-bpy)]PF$_6$ (**3**)	0.663 ± 0.060	1.68 ± 0.52
[Ir(Cl-ptpy)$_2$(Cl$_2$-bpy)]PF$_6$ (**4**)	0.609 ± 0.098	2.00 ± 0.52
Cisplatin	4.14 ± 0.31	23.03 ± 0.25

It is found that all complexes exhibit appreciable cytotoxicity against the two cell lines with IC$_{50}$ values ranging from 0.4 µM to 2.4 µM. The highest activity was observed for **1**, which exhibits a 10-fold higher activity towards both cell lines than the clinical drug cisplatin.

In a previous work, we have investigated similar cyclometalated complexes, in which the bipyridine moiety was substituted by a phenanthroline unit.[17] In accordance with these previously tested compounds, the MCF-7 cells show lower sensitivity to the compound treatments than the HT-29 cells. The complexes show similar cytotoxic activity compared to their phenanthroline analogues with the exception of having slightly higher IC$_{50}$ values for MCF-7 cells. All in all, all compounds exhibit a strong cytotoxic activity in the high nanomolar/ low micromolar range with no significant difference in the cytotoxic behavior between the two metals in this specific ligand system. These initial biological studies illustrate the high antiproliferative potential of our complexes emphasising the suitability of cyclometalated iridium and rhodium complexes as new promising anti-cancer agents.

4. Conclusions

The syntheses, photophysical properties, and biological activity of four new bis-cyclometalated cationic complexes [M(C^N)$_2$(4,4'-Cl$_2$bpy)]PF$_6$ (M = Rh; Ir; C^N = ptpy, Clppy) are reported. Crystal and molecular structures of the new complexes were confirmed by X-ray crystal structure determination Iridium complexes **2** and **4** are luminescent in solution and in polymer matrices at ambient temperature. The emission assigned to a ^{3}MLCT state strongly depends on the environment. In a rigid polymer matrix (PMMA), [Ir(ptpy)$_2$(4,4'-Cl$_2$bpy)]$^+$ (**2**) and [Ir(5-Cl-ppy)$_2$(4,4'-Cl$_2$bpy)]$^+$ (**4**) show moderately strong yellow luminescence whereas in solution (CH$_2$Cl$_2$) the emission is significantly red shifted. The emission quantum yield ϕ_{PL} and decay time τ_{em} values are significantly larger in rigid PMMA than in liquid solution due to different efficiency of non-radiative relaxations to the ground state. This rigidochromic behavior is accounted for distinctly different stabilization of the ^{3}MLCT-excited state in flexible solution and quasi-solid polymer films. All compounds exhibit cytotoxic effects towards two cell lines (HT29 and MCF-7).

Acknowledgments

The authors are grateful to the Department of Chemistry of the Ludwig Maximilians University Munich for support. P. Mayer is acknowledged for collecting the X-ray crystal data and Ms. Mahboubeh Jamshidi (University Regensburg) is acknowledged for her assistance with photophysical measurements. The *Johnson Matthey plc*, Reading, UK, is gratefully acknowledged for a generous loan of hydrated iridium chloride.

Supplementary material

CCDC-1528482 (**1**) and –1528483 (**4**) contain the supplementary crystallographic data for this paper. These data can be obtained free of charge from The Cambridge Crystallographic Data Centre via http://www.ccdc.cam.ac.uk/data_request/cif.

References

---

[1] (a) C.-H. Lin, Y.-C. Chiu, Y. Chi, Y.-T. Tao, L.-S. Liao, M.-R. Tseng, G.-H. Lee, Organometallics 31 (2012) 4349 and references therein;
(b) S.-K. Leung, K.Y. Kwok, K.Y. Zhang, K. K.-W. Lo, Inorg. Chem. 49 (2010) 4984 and references therein;
(c) H. Yersin, A. F. Rausch, R. Czerwieniec, T. Hofbeck, T. Fischer, Coord. Chem. Rev. 255 (2011) 2622 and references therein;
(d) K. K.-W. Lo, K. Y. Zhang, RSC Advances 2 (2012) 12069-12083;
(e) B. Minaev, G. Baryshnikov, H. Agren, Phys. Chem. Chem. Phys. (2013) DOI: 10.1039/C3CP53806K and references therein.

[2] a) R.D. Costa, E. Orti, H.J. Bolink, S. Graber, S. Schaffner, M. Neuburger, C.E. Housecroft, E.C. Constable, Adv. Funct. Mater. 19 (2009) 3456;
b) R.D. Costa, E. Orti, D. Tordera, A. Pertegas, H.J. Bolink, S. Graber, C.E. Housecroft, L. Sachno, M. Neuburger, E.C. Constable, Adv. Energy Mater. 1 (2011) 282;
c) R.D. Costa, E. Orti, H.J. Bolink, S. Graber, C.E. Housecroft, E.C. Constable, Chem. Commun. 47 (2011) 3207

[3] a) M. Schmittel, H. Lin, Inorg. Chem. 46 (2007) 9139
b) H. Lin, M.E. Cinar, M. Schmittel, Dalton Trans., 39 (2010) 5130;
c) P-K. Lee, W.H-T. Law, H-W. Liu, K. K-W. Lo, Inorg. Chem. 2011, 50, 8570;
d) B.B.H. Leavens, C.O. Trindle, M. Sabat, Z. Altun, J.N. Demax, B.A. DeGraff, J. Fluoresc. 22 (2012) 163.

[4] A. Valore, E. Cariati, C. Dragonetti, S. Righetto, D. Roberto, R. Ugo, F. DeAngelis, S. Fantacci, A. Sgamellotti, A. Macchioni, D. Zuccaccia, Chem. Eur. J. 16 (2016), 4814.

---

[5] For a review on bioactive iridium and rhodium complexes as therapeutic agents see: C-H. Leung, H-J. Zhong, D. S-H. Chan, D-L. Ma, Coord. Chem. Rev. 257 (2013) 1764, and references cited therein.

[6] C.-H. Leung, H.-J. Zhong, H. Yang, Z. Cheng, D. S.-H. Chan, V. P.-Y. Ma, R. Abagyan, C.-Y. Wong, D.-L. Ma, Angew. Chem. 124 (2012) 9144 ; Angew. Chem. Int. Ed. 51 (2012) 9010.

[7] (a) P.-K. Lee, H.-W. Liu, S.-M. Yiu, M.-W. Louie, K. K.-W. Lo, Dalton Trans. 40 (2011) 2180.

[8] K. K.-W. Lo, C.-K. Li, K.-W. Lau, N. Zhu, Dalton Trans. (2003) 4682.

[9] K. Qiu, Y. Liu, H. Huang, C. Liu, H. Zhu, Y. Chen, L. Ji, H. Chao, Dalton Trans. 45 (2016) 16144

[10] a) U. Mäder, T. Jenny, A. von Zelewsky, Helv. Chim. Acta, 69 (1986) 1085;
b) A. Zilian, U. Maeder, A. von Zelewski, H.U. Güdel, J. Amer. Chem. Soc. 111 (1989) 3855;
c) U. Maeder, A. von Zelewsky, H. Stoeckli-Evans, Helv. Chim. Acta,75 (1992) 1320;

[11] A. P. Wilde, K.A. King, R.J. Watts, J. Phys. Chem. 95 (1991) 629

[12] K.P. Balashev, M.V. Puzyk, E.V. Ivanova, Russ. J. Gen. Chem. 81 (2011) 1547

[13] a) C. Dragonetti, L. Falciola, P. Mussini, S. Righetto, D. Roberto, R. Ugo,, A. Valore, F. De Angelis, S. Fantacci, A. Scamellotti, M. Ramon, M. Muccini, Inorg. Chem. 46 (2007) 8533;
b) E.C. Constable, C.E. Housecroft, P. Kopecki, C.J. Martin, I.A. Wright, J.A. Zampese, H.J. Bolink, A. Pertegas, Dalton Trans. 42 (2013) 8086;
c) M. Sarma, T. Chatterjee, R. Bodapati, K.N. Krishnakanth, S. Hamad, S.V. Rao, S.K. Das, Inorg. Chem.55 (2016) 3530.

[14] a) M.S. Lowry, W.R. Hudson, R.A. Pascal, Jr., S. Bernhard, J. Am. Chem. Soc. 126 (2004) 14129;
b) J.I. Goldsmith, W.R. Hudson, M.S. Lowry, T.H. Anderson, S. Bernhard, J. Am. Chem.Soc. 127 (2005) 7502.

[15] (a) M. Graf, H.-C. Böttcher, K. Sünkel, Inorg. Chim. Acta 394 (2013) 363;
(b) H.-C. Böttcher, M. Graf, K. Sünkel, P. Mayer, H. Krüger, Inorg. Chim. Acta 365 (2011) 103;
(c) H.-C. Böttcher, M. Graf, K. Sünkel, H. Krüger, Inorg. Chim. Acta 370 (2011) 523;
(d) H.-C. Böttcher, M. Graf, K. Sünkel, B. Salert, H. Krüger, Inorg. Chem. Commun. 14 (2011) 377;
(e) K. Sünkel, M. Graf, H.-C. Böttcher, B. Salert, H. Krüger Inorg. Chem. Commun. 14 (2011) 539;
(f) M. W. Thesen, H. Krüger, S. Janietz, A. Wedel, M. Graf, J. Polym. Sci., Part A: Polym. Chem. 48 (2010) 389;
(g) M. Graf, M. Thesen, H. Krüger, P. Mayer, K. Sünkel, Inorg. Chem. Commun. 12 (2009) 701;
(h) M. W. Thesen, H. Krüger, S. Janietz, A. Wedel, M. Graf, J. Polym. Sci., Part A: Polym. Chem. 48 (2010) 389.

[16] (a) M. Graf, K. Sünkel, Inorg. Chim. Acta 371 (2011) 42;
(b) M. Graf, K. Sünkel, Inorg. Chim. Acta 379 (2011) 40;
(c) M. Graf, K. Sünkel, Inorg. Chim. Acta 387 (2012) 81.

[17] M. Graf, Y. Gothe, N. Metzler-Nolte, R. Czerwieniec, K. Sünkel, J. Organomet. Chem., 765 (2014) 46.

[18] P.E.A. Ribeiro, C.L. Donnici, E.N. dos Santos, J. Organomet. Chem. 691 (2006) 2037.

---

[19] F.R. Pavan, G.V. Poelhsitz, M.L.F. Barbosa, S.R.A. Leite, A.A. Batista, J. Ellena, L.S. Sato, S.G. Franzblau, V. Moreno, D. Gambino, C.Q.F. Leite, Eur.J.Med.Chem. 46 (2011), 5099.

[20] F. Hildebrand, Ch. Kohlmann, A. Franz, St. Lütz, Adv. Synth. Catal. 350 (2008) 909.

[21] WINGX: L. J. Farrugia, J. Appl. Crystallogr. 32 (1999), 837-838;
PLATON: A. L. Spek, J. Appl. Crystallogr., , 36 (2003), 7-13;
SHELXL: G. M. Sheldrick, Acta Cryst. A64 (2008) 112-122; Acta Cryst. C71, (2015), 3-8; doi: 10.1107/S2053229614024218

[22] (a) A. D. Becke, J. Chem. Phys., 98 (1993), 5648-5652.
(b) P. J. Stephens, F. J. Devlin, C. F. Chabalowski, M. J. Frisch, J. Phys. Chem. 98, (1994)**,** 11623-11627.

[23] A. Schaefer, H. Horn, R. Ahlrichs, J. Chem. Phys., 97 (1992) 2571.

[24] F. Weigend, R. Ahlrichs, Phys. Chem. Chem. Phys., 7 (2005) 3297.

[25] a) P. J. Hay, W. R. Wadt, J. Chem. Phys., 82 (1985) 270;
b) P. J. Hay, W. R. Wadt, J. Chem. Phys., 82 (1985) 299.

[26] Gaussian09W, Version 8.0, M. J. Frisch, G. W. Trucks, H. B. Schlegel, G. E. Scuseria, M. A. Robb, J. R. Cheeseman, G. Scalmani, V. Barone, B. Mennucci, G. A. Petersson, H. Nakatsuji, M. Caricato, X. Li, H. P. Hratchian, A. F. Izmaylov, J. Bloino, G. Zheng, J. L. Sonnenberg, M. Hada, M. Ehara, K. Toyota, R. Fukuda, J. Hasegawa, M. Ishida, T. Nakajima, Y. Honda, O. Kitao, H. Nakai, T. Vreven, J. A. Montgomery, Jr., J. E. Peralta, F. Ogliaro, M. Bearpark, J. J. Heyd, E. Brothers, K. N. Kudin, V. N. Staroverov, R. Kobayashi, J. Normand, K. Raghavachari, A. Rendell, J. C. Burant, S. S. Iyengar, J. Tomasi, M. Cossi, N. Rega, J. M. Millam, M. Klene, J. E. Knox, J. B. Cross, V. Bakken, C. Adamo, J. Jaramillo, R. Gomperts, R. E. Stratmann, O. Yazyev, A. J. Austin, R. Cammi, C. Pomelli, J. W. Ochterski, R. L. Martin, K. Morokuma, V. G. Zakrzewski, G. A. Voth, P. Salvador, J. J. Dannenberg, S. Dapprich, A. D. Daniels, Ö. Farkas, J. B. Foresman, J. V. Ortiz, J. Cioslowski, and D. J. Fox, Gaussian, Inc., Wallingford CT, 2009.

[27] F. DeAngelis, L. Belpassi, S. Fantacci, J.Mol.Struct. THEOCHEM 914 (2009) 74.

[28] S. Ladouceur, D. Fortin, E. Zysman-Colman, Inorg. Chem. 50 (2011) 11514.

[29] Y. Ohsawa, S. Sprouse, K. A. King, M. K. DeArmond, K. W. Hanck, R. J. Watts, J. Phys. Chem. 91 (1987) 1047.

[30] F. Gärtner, D. Cozzula, S. Losse, A. Boddien,G. Anilkumar, H. Junge, T. Schulz, N. Marquet, A. Spannenberg, S. Gladiali, M. Beller, Chem. Eur. J. 17 (2011) 6998

[31] K. K.-W. Lo, K. Y. Zhang, C.-K. Chung, K. Y. Kwok, Chem. Eur. J. 13 (2007), 7110.

[32] www.chemisian.com

[33] R. L. Martin, J. Chem. Phys. 118 (2003) 4775.

[34] A. F. Rausch, H. H. H. Homeier, H. Yersin, Top. Organomet. Chem. 29 (2010) 193.

[35] D. Mochizuki, M. Sugiyama, M. M. Maitani, Y. Wada, Eur. J. Inorg. Chem. (2013) 2324

[36] M. Graf, K. Sünkel, R. Czerwieniec, H.-C. Böttcher, J. Organomet. Chem. 745-746 (2013) 341.

[37] J. V. Caspar, T. J. Meyer, J. Phys. Chem. 87 (1983) 952.

Highlights

- 4 new bis-cyclometalated Rh and Ir complexes with 4,4‘-Cl_2BiPy are described
- Crystal structures of [M(C^N)$_2$(4,4’Cl_2BiPy)] (M=Rh,Ir) are reported
- All complexes show antiproliferative activity against certain cancer cells
- The Ir complexes are strong yellow emitters in PMMA matrix